


 Cite this: *Green Chem.*, 2025, **27**, 4611

Industrial-scale biorefinery for *n*-caproate production from food waste†

 Junjie Qiu,^a Yujie Wang,^a Fan Lü,^{a,b} Nanling Liao,^a Jing Li,^a Xiao Hua,^a Hua Zhang,^{a,b} Bin Xu^{a,b} and Pin-Jing He^{a,b}

Food waste contributes nearly 10% of global carbon emissions, with over one billion tonnes produced annually. Carbon chain elongation (CCE) technology converts bio-waste into biochemicals *via* microbial catalysis. Here, we present an industrial-scale biorefinery plant to produce *n*-caproate from food waste. This plant can stably produce green *n*-caproate from food waste at atmospheric temperatures without added chemicals and heat energy. Gibbs free energy analysis demonstrated the underlying biochemical reactions of the CCE system, and techno-economic evaluation showed reduced operational cost and greenhouse gas emission due to avoidable chemicals and heat energy. Since the residual broth from the extraction of *n*-caproate can be employed as an alternative carbon source for nitrogen removal in wastewater treatment, a theoretical model was proposed to estimate the concentrations of residual dissolved organic nitrogen in the effluent. This industrial-scale biorefinery for *n*-caproate would offer a closed-loop system for the sustainable cascade management of food waste.

 Received 31st December 2024,
Accepted 17th March 2025

DOI: 10.1039/d4gc06592a

rsc.li/greenchem

Green foundation

1. This work presents the first industrial-scale biorefinery plant to produce *n*-caproate from food waste at atmospheric temperatures without added chemicals and heat energy. The successful industrial-scale biorefinery plant for green *n*-caproate offers a closed-loop system for the sustainable and cascade management of food waste.
2. The integrated system to gear the anaerobic bio-membrane reactor and micro-aeration technology could simultaneously suppress propionic acid fermentation as a competitive reaction, and ammonify the proteins to avoid the addition of NaOH.
3. The avoidable input of NaOH, ethanol and heat energy can offset the high cost in the purification of *n*-caproate, so the industrial-scale purification of *n*-caproate needs to be taken up in the future.

Introduction

Over one billion tonnes of food waste were generated in 2022, and contributed approximately 8%–10% of global greenhouse gas emissions.^{1,2} Reduction of food loss is the top priority strategy, but food waste is inevitable.^{3,4} Sustainable management of food waste is an essential topic,⁵ which will evolve from the generation of bioenergy to the production of chemical energy,^{6,7} because greener energy transition in the future⁸ will reduce the carbon credits from energy recovery. Volatile

organic acids are important in both edible and inedible applications.^{9,10} Previous studies mainly focused on the production of C₁–C₃ organic acids from food waste.¹¹ Steinbusch *et al.*¹² and Agler *et al.*¹³ proposed carbon chain elongation (CCE) technology to upgrade C₁–C₃ fermentation products to C₆–C₈ fossil-free chemicals derived from bio-waste. *n*-Caproate is a versatile and important chemical intermediate, used in the production of flavour additives, lubricants, plasticizers, feed additives, antimicrobial agents and other products.^{12,14} Meanwhile, the conventional production of medium chain fatty acid is achieved by extraction from natural biomass resources (*e.g.*, palm kernel oil, coconut oil, *etc.*)^{15,16} or chemical synthesis.⁹ Therefore, the production of *n*-caproate from food waste is a promising and green strategy for both food waste management and *n*-caproate production in terms of the zero-carbon future and circular economy.

CCE to *n*-caproate was proven to occur *via* reverse β -oxidation (RBO) pathways,^{12,17} which can be mediated by various electron donors, such as H₂ (C₀),¹⁸ CO (C₁),¹⁹ ethanol

^aInstitute of Waste Treatment and Reclamation, College of Environmental Science and Engineering, Tongji University, Shanghai, 200092, PR China.

E-mail: solidwaste@tongji.edu.cn

^bShanghai Institute of Pollution Control and Ecological Security, Shanghai, 200092, PR China

† Electronic supplementary information (ESI) available: Detailed information of experiments, eqn (S1–S8), Fig. S1–S8, Tables S1–S3. See DOI: <https://doi.org/10.1039/d4gc06592a>



(C₂)¹³ and lactate (C₃).²⁰ In this regard, ChainCraft (<https://chaincraft.com/technology/>) and Capro-X, Inc. (<https://www.capro-x.com/>) have operated a pilot- or demonstration-scale plant by using ethanol as an intermediate. Typically, starch is the main fraction of food waste.^{21,22} Monosaccharide hydrolysed from starch can be converted to ethanol and lactate as CCE electron donors with identical carbon utilisation efficiency, because one third of CO₂ is lost during the ethanol fermentation of glucose or CCE of lactate (details in Table S1†). Acetyl-coenzyme A (acetyl-CoA) is the key compound for RBO reactions.^{23,24} Fermented ethanol was easily oxidised to acetate mediated by acetyl-CoA to consume nicotinamide adenine dinucleotide (NADH), so the ethanol/acetate ratio is typically excessive by extra addition.^{25,26} Addition of external ethanol is estimated to be the major contributor to the environmental impact.²⁷ The other problem is that lactate would be oxidised to propionate as a competitive reaction to inhibit CCE metabolism.²⁰ Therefore, it is challenging to select appropriate intermediates to modulate CCE pathways, and avoid the abovementioned competitive transformation of electron donors for continuous production of *n*-caproate from food waste other than first- or second-generation biomass resources.

CCE from food waste typically occurs in an open culture system to reduce cost and greenhouse gas emissions from sterilisation compared with the common food fermentation industry. Enrichment of functional microbes for CCE is another bottleneck in an open culture system due to the slow growth rate and competition with methanogenic microorganisms. Bench-scale reactors can be applied in various types of reactors, including upflow anaerobic filters,²³ upflow anaerobic sludge blankets,²⁰ and embedded beads²⁸ to separate the hydraulic retention time and solid retention time. However, the production of *n*-caproate from food waste cannot be applied with these types of reactors with high solid concentrations of input food waste. Large amounts of bases and acids are usually consumed to maintain the pH value of the CCE reactor at 5–6 to inhibit methanogenesis without the addition of expensive sodium 2-bromoethanesulfonate²⁹ or regulation by H₂ partial pressure.¹⁸ Additionally, the conventional temperature for CCE is 35 °C, so heat energy (*e.g.*, saturated steam) shall be provided in the industrial-scale system. The consumption of chemicals and steam would diminish the significance of carbon emission reduction for bioconversion of bio-waste to biochemicals as well.²⁷ Generally, issues, which still need to be addressed to realise the industrial-scale production of *n*-caproate from food waste, include coupling hydrolysis, primary fermentation and CCE reactions in different units, enrichment of functional microbes, and decreasing consumption of added chemicals and heat energy.

In the present study, an industrial-scale biorefinery plant was successfully commissioned to produce *n*-caproate from food waste. The study showed that the CCE system conducted concurrent reactions involving CCE of lactate and ethanol, along with ammonification of protein fractions, without pH control and external heating. The performance and pathways of industrial-scale CCE production from food waste were

shown by material flow analysis and Gibbs free energy analysis by solving contradictory equations. Besides the purification of *n*-caproate, the viability of mixed medium chain fatty acids (MCCAs) used as an extra carbon source for denitrification in various biological wastewater treatment plants (WWTP) was evaluated by a theoretical model to determine the concentrations of dissolved organic nitrogen (DON) in effluents. Furthermore, a comprehensive techno-economic evaluation estimated the performance of industrial-scale production of *n*-caproate for sustainable management of bio-waste.

Results and discussion

General performance of the industrial-scale biorefinery plant for *n*-caproate production

The typical composition of food waste as feedstock is shown in Fig. S1.† The fraction of inedible food can be up to 97% due to the source separation policy in China as the favourable stocks of the biorefinery plant. Food waste comprises more than half of municipal solid waste in China as well as other developing countries.⁴ As an average performance, 116–132 t d⁻¹ broth was produced by mixing MCCAs in the broth after the ultrafilter unit, and 15.5 t d⁻¹ impurities with a water content of approximately 60% were isolated from the pre-treatment section.

Performance of the pre-treatment section

In the pre-treatment section, the effluent of Decanter I was continuously recirculated to the depackage unit to avoid clogging in Fig. 1. Carbohydrates, which are one of the main fractions in food waste, are easily converted to lactate and ethanol during the transport process through homolactic and ethanol fermentation. It was analogous to a previous study.²¹ Therefore, the concentrations of organic acids and ethanol were similar in the effluent of the depackage unit (EDep), effluent of the crusher unit (EC), effluent of the gravity separation unit (EGS) and Slurry in Fig. S2† with an average of 273 mM lactate and 90 mM ethanol, corresponding to 73% and 8% of dissolved organic carbon (DOC), which offer sufficient electron donors for CCE reactions. The pre-treatment section mainly involved a physical treatment to increase digestibility by microbes and enzymes, and the chemical composition of feedstock remained constant.

Performance of the CCE section

After the CCE section, the concentration of *n*-caproate can be 59–71 mM [*i.e.*, 8.0 g L⁻¹, 17.6 g chemical oxygen demand (COD) per L], and the average value was 66 mM, corresponding to an average yield ratio of 35% in terms of influent DOC. The lactate mediated *n*-caproate production was almost complete in Reactor I, as reflected by Fig. S2,† because recirculation from Reactors II and III to Reactor I was not in use in this scenario. The efficiency of *n*-caproate production could be up to 3.8 kg-*n*-caproate per (m³ d) [*i.e.*, 8.36 kg COD-*n*-caproate per (m³ d)] in Reactor I, confirming that the performance of *n*-caproate production in this industrial-scale plant was comparable to the bench-scale²⁰ or pilot-scale reactors^{30,31} that



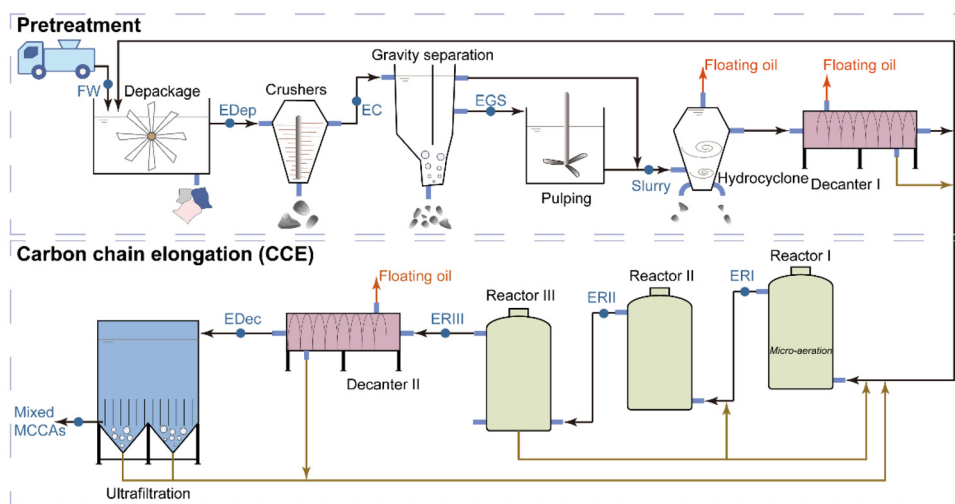


Fig. 1 Detailed workflow of the industrial-scale biorefinery plant for the production of *n*-caproate from food waste with a capacity of 150 t d⁻¹. The sampling sites includes food waste (FW), effluent of the depackage unit (EDep), effluent of the crusher unit (EC), effluent of the gravity separation unit (EGS), slurry, effluent of ECC reactor I (ERI), effluent of ECC reactor II (ERII), effluent of ECC reactor III (ERIII), effluent of the decanter I (EDec), mixed MCCAs from the ultrafiltration unit and storage tanks. The floating oil is mainly edible oil in the food waste, which was sold as the feedstock of crude biodiesel.

produced *n*-caproate from lactate (Table 1). The net yield of *n*-caproate was 7.2 kg per t-food waste (*i.e.*, 0.12 kg per kg VS), and 0.8 kg-*n*-caproate per tonne food waste was lost in the impurities from the pre-treatment section. The average yields of *i*-caproate and heptylate were 1.4% and 5.2%, respectively. The remaining DOC was 10% of acetate and 14.2% of butyrate, and the odd-numbered organic acids were less than 5%. Caprylate and other longer carbon-chain organic acids were not detected. The production of *n*-caproate mediated by lactate would release one third of CO₂ according to the stoichiometric number of CCE reactions in Table S1.[†] Whereas, the DOC concentrations after the CCE reactors were similar to the broth in the pre-treatment sections in Fig. S3.[†] Concurrently, dissolved nitrogen (DN) increased to 2000–2500 mg L⁻¹ from 1000–1200 mg L⁻¹ as shown in Fig. S4.[†] This indicated that approximately 21% of extra DOC was further hydrolysed into the broth in Reactors I, II and III. pH increased to 5.8–5.9 from 3.8–3.9 after CCE reactions shown in Fig. S5.[†]

Concurrent reactions involving CCE of lactate and ethanol, along with ammonification of protein fractions

Food waste contains various fractions, including carbohydrate, proteins and lipids.²² Therefore, the pathways for the pro-

duction of *n*-caproate from food waste are fairly complicated to involve various compounds such as C₂–C₈ alcohols, and normal and branched carboxylates.^{25,29,32} Thereby, Gibbs free energy analysis by solving contradictory equations was applied to investigate this complex engineering system. Totally, eight reactants and products were detected in the CCE section, and seven most probable reactions were selected in Fig. 2A to show the CCE reactions mediated by lactate and ethanol. The fitted results were in perfect agreement with the realistically changed number of substances in the CCE reaction, except for 14% inaccuracy for the fitted results of lactate, which showed satisfactory fitting performance. Additionally, 2–10 mM *i*-C₄–C₆ may be generated from the unidentified 14% of lactate, but the generation of branched carboxylates was typically difficult.²⁵ Lactate and ethanol are firstly converted to acetyl-CoA and then enter the RBO pathways³³ through reaction 1 in Fig. 2B, along with generating 1 mol-CO₂ per mol-reaction. 28.6% of carbon in lactate was converted to CO₂ in Fig. 3, which was lower than the theoretical carbon efficiency of 33.3% for *n*-caproate production. This confirmed that some of the lactate intermediates remained in the form of acetate and butyrate, or entered propionic acid fermentation as a competitive reaction.³⁴ 43% of lactate was initially oxidised to acetate

Table 1 Comparison of manufacturing processes with previous studies regarding CCE mediated by lactate

Feedstock	Scale	Max <i>n</i> -caproate production rate [kg (m ³ d ⁻¹) ⁻¹]	Max <i>n</i> -caproate concentrations (mM)	pH	Ref.
<i>l</i> -Lactate and <i>n</i> -butyrate	0.37 L d ⁻¹	3.1	Online extraction	5	20
Food waste	0.3–1 L (Batch)	1.9	47	4.8 (add NaOH)	31
Acid whey wastewater	0.1–0.2 L d ⁻¹	3.2	90	5.5 (add NaOH)	16
Food wastewater	33–167 L d ⁻¹	26.4	170	6.0 add hydroxide	35
Food waste	150 t d ⁻¹	3.8	71	5.5 without NaOH addition	This work



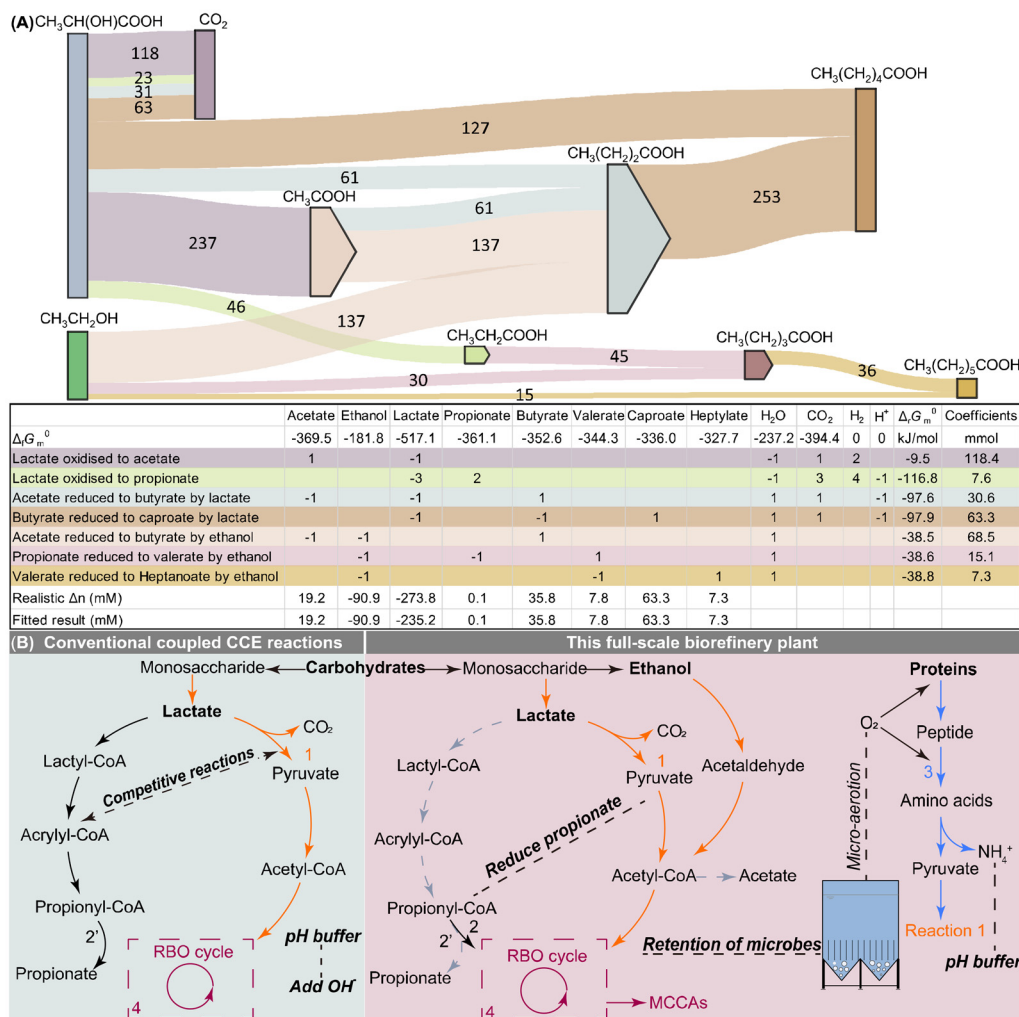


Fig. 2 Pathways of MCCA production from food waste mediated by endogenous ethanol and lactate (A). The numbers on the Sankey diagram are the reaction coefficients in terms of carbon (mM) based on the average results of Fig. S2.† Concurrent reactions including CCE from food waste and ammonification of protein fractions enhanced by micro-aeration (B). Coenzyme A (CoA) is the key coenzyme in CCE metabolism.

with a low $\Delta_r G_m^0$ value of -9.5 kJ mol^{-1} , and they were subsequently coupled with the CCE reaction by 34% of lactate. Additionally, the theoretical carbon efficiency is identical to that in the production of *n*-caproate from carbohydrate ($\text{C}_6\text{H}_{12}\text{O}_6$)_n mediated by lactate and ethanol, but $\Delta_r G_m^0$ of CEE from lactate is lower than that from ethanol according to Table S1.† Thereby, 75% of ethanol affords NADH through oxidised acetyl-CoA to reduce acetate to butyrate. Generally, *n*-caproate was produced stably in these CCE reactors.

Propionate accumulation was the most probable competitive reaction (reaction 2' in Fig. 2B) to generate propionyl-CoA to inhibit CCE reactions, and wasted the electron donor, especially within a high organic load rate $>15 \text{ kg COD per (m}^3 \text{ d)}$ in Fig. 2B as the conventional CCE reactions,²⁰ whereas the generated propionate was further reduced to valerate and heptanoate through reaction 2 as shown in Fig. 2B,²⁶ consequently diminishing the side reaction of propionic fermentation from lactate. It was previously observed in a bench-scale reactor,

where the higher yield rate of *n*-caproate was consistent with the higher concentration of ethanol.¹⁶ Therefore, only 2.7% of lactate was estimated to enter the propionic fermentation, and 0.1 mM propionate was net produced as shown in Fig. 2A. The microbiological mechanism of this phenomenon would be worth further investigation in the bench-scale reactor.

n-Caproate production in this biorefinery plant was apparently attributed to the collaborating microbes of *Olsenella* and *Lachnospiraceae*, which hold the abundance of amplicon sequence variants up to 24% and 29% after a one-year long-term commissioning shown in Fig. S7,† respectively. *Lachnospiraceae* could provide acetate and butyrate^{36,37} for *Olsenella* to produce *n*-caproate.^{16,35} Compared to *Caproiciproducens*,³⁸ the abundance of *Olsenella* was typically low or absent in lactate-fed CCE reactors.^{28,31,35} In this micro-aerobic membrane reactor, the solid retention time was approximately 120–200 days by controlling the concentrations of total solid (TS) less than 13 g L^{-1} . The ultrafiltration unit



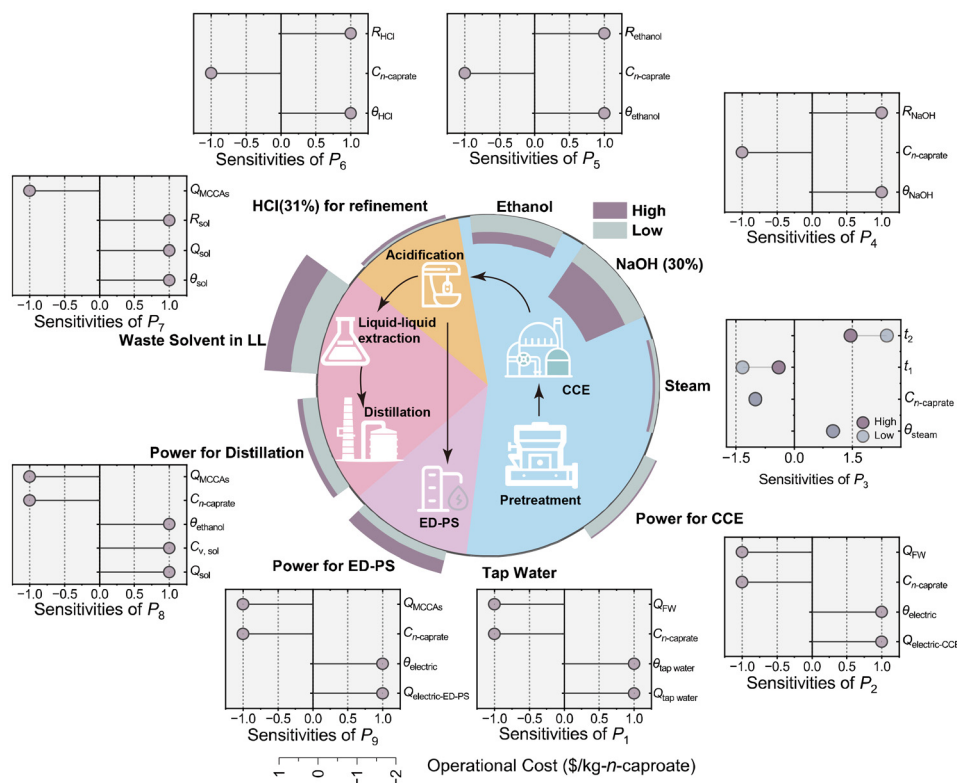


Fig. 3 Techno-economic evaluation and sensitivity analysis for the industrial-scale biorefinery plant and the potential operational cost of refinement and purification of *n*-caproate. P1–P9 are the operation costs, and the detailed calculation processes are shown in the ESI.†

retained the CCE functional microbes as the core unit of the CCE section. More interestingly, the cooperation of *Olsenella* and Lachnospiraceae with the abundance up to 50% can still work at a temperature of 10–15 °C in Fig. S8,† and the concentrations of *n*-caproate still could be up to 55 mM with the continuous recirculation of Reactors II and III to Reactor I. The *n*-caproate production efficacy could be 1.05 kg *n*-caproate per (m³ d) [*i.e.*, 2.32 kg COD-*n*-caproate per (m³ d)] at such temperatures. It suggested the significant importance of the cooperation of *Olsenella* and Lachnospiraceae as a novel pair of model microbes for CCE reactions, and contributed to the flexible *n*-caproate production without heating in this industrial-scale plant. Additionally, this CCE system was commissioned without external inoculum, implying a stable microbial community.

The remnant O₂ in the concentrated CCE microbes was recirculated to Reactor I, maintaining the dissolved oxygen at 0.02–0.3 mg L⁻¹ in Reactor I in Fig. 1 and 2B. The micro-aeration process is well-acknowledged to enhance the hydrolysis process in the anaerobic process,^{39,40} as reflected by reaction 3 in Fig. 2B. The hydrolysed amino acids simultaneously offer the buffer capacity in the form of NH₃-N, and acetyl-CoA from pyruvate for reaction 1 in Fig. 2B. After the CCE section, NH₄⁺-N dramatically increased to 1500–2100 mg L⁻¹ from 260–280 mg L⁻¹ in Fig. S4,† which has also been reported as a positive condition for *n*-caproate production.⁴¹ Ammonia was

generated from amino acids, and transformed into ammonium at pH 5.8–5.9. It corresponded to 88–130 mM NH₄⁺-N in Reactors I, II, and III, which can be compared to 0.38–0.56 mmol-OH⁻ per mmol organic acid in this weak acid buffer system to replace the OH⁻ dosage (Table 1).^{16,27,28,42} Overall, this CCE reactor was shown to be an integrated system to gear the anaerobic bio-membrane reactor and micro-aeration technology, contributing to concurrent high production of *n*-caproate from lactate, reduction of propionate by ethanol, and ammonification of proteins.

Techno-economic evaluation: purification of mixed MCCA into chemicals

This biorefinery plant can produce *n*-caproate from food waste without heat energy and chemical addition of NaOH, ethanol, and sodium 2-bromoethanesulfonate through CCE reactions, compared to previous bench- or pilot-scale studies.^{20,31,35} The direct operating costs of pre-treatment section included the cost of tap water for cleaning and electricity for pre-treatment of food waste, and those of the pre-treatment section were only electricity for crossflow washing in the ultrafiltration unit, where costs for offline cleaning of the ultrafiltration unit can be omitted. Totally, this corresponded to 0.32–0.36 \$ per kg *n*-caproate without the depreciation of equipment cost in Fig. 3. The reduction of chemicals and heat energy can save 1.1–2.6 \$ per kg *n*-caproate without considering 2-bromoetha-



nesulfonate, which reduces cost by 70–90%. Additionally, sensitivity analysis showed the operating costs of electricity and tap water were negatively correlated with the concentration of *n*-caproate in the broth. The TS in this case was fairly low at 6%–10% due to inevitable addition of cleaning water during transport. A higher concentration of produced *n*-caproate can further reduce operational costs, as reflected by sensitivity analysis. Accordingly, previous life cycle analysis showed consumption of ethanol, and NaOH also contributed 40–45% of global warming potential per kg *n*-caproate (*i.e.*, 4–5 kg CO₂ per kg *n*-caproate) from the fermentation to the purification.²⁷ A green carbon footprint of *n*-caproate production in this biorefinery plant was demonstrated.

For the industrial-scale plant, the CCE reactor coupling with online separation was not chosen because a complicated engineering system is more likely to go wrong. Therefore, biological fermentation and refinement units were isolated as tandem units, and the filtered broth from the CCE section was directly used as the extra carbon source without phase separation for now. The refinement and purification of *n*-caproate can be conducted by conventional and novel separation technologies shown in Fig. 3. First, the broth should be acidified to make *n*-caproate in the undissociated form, which would cost 0.05–0.14 \$ per kg *n*-caproate. The electro dialysis phase separation (ED-PS) process (0.23–0.58 \$ per kg *n*-caproate) is shown to be obviously cheaper than liquid–liquid extraction tandem with the distillation (LL-D) process (1.1–1.9 \$ per kg *n*-caproate) without the depreciation of equipment. It can be estimated that operational expenditure associated with the refinement and purification processes can be offset by reduced cost incurred in the pre-treatment and CCE sections, making the production of *n*-caproate from food waste sustainable.

Application of mixed MCCAs as a carbon source in WWTP

The fermented broth shall be recovered in the cascade to offer closed-loop management of food waste. After the separation of high valued *n*-caproate, the residual broth can also be used as an extra carbon source for nitrogen removal. MCCAs in the filtered broth can be either subjected to further refinement and purification as chemicals or direct applications as an alternative to the extra carbon source in WWTP. Therefore, the ratio of f_{DON} (*i.e.*, NH₄⁺-N/DN) can be up to 0.8–1.0 from 0.22–0.28 along with the CCE reactions, showing a high ammonification rate along with the CCE reactions. Additionally, the concentration of PO₄³⁻-P in pre-treatment and CCE processes was 100–360 mg L⁻¹ due to the typical low phosphorus fraction in food waste.²² It corresponds to a ratio of NH₄⁺-N/PO₄³⁻-P of 6–10, which is suitable for microbial growth in WWTP without enhanced biological phosphorus removal.⁴³

However, the ammoniated dissolved organic nitrogen (DON) would have a negative impact on the performance of WWTP, because DON cannot be removed in a common WWTP by using activated sludge.^{44,45} The COD/N of filtered broth was 20–25 with an f_{DON} value of 0.8–1.0, and COD/N of extracted broth would be decreased to approximately 15 by the ED-PS process. Additionally, potential $\{\Delta\text{TN}_{\text{eff}}\}_{\text{min}}$ [estimated

increased concentration of total nitrogen (TN) in the effluent of WWTP] would be further higher if the residual broth was applied to steel industrial wastewater and mature leachate treatment, because the dosage α can be up to 3%–5%. It would exert little impact on sewage wastewater treatment ascribed to the undegradable DON shown in Fig. 4. The nitrification–denitrification process with the lower f_{dn} is less vulnerable than nitrification–denitrification, but the latter is more common. The LL-D process does not change the COD/N of extracted broth, because the wasted solvent is left in residual broth. A typical loss ratio of solvent is 0.5%–1%,^{27,35} suggesting that easily biodegradable solvent is recommended for the refinement of *n*-caproate.

Fig. 2A shows that approximately 20% of organic acids were released in the form of CO₂ during the CCE reaction. Actually, CCE reactions do not consume electrons, because electrons would be stored in the final electron acceptor (*i.e.*, mixed MCCAs). Additionally, fermentation of acetate from lactate resulted in the loss of one-third of electrons in the form of CO₂ in reactors I, II, and III, but a typical f_{dn} value of acetate and lactate is 3.4 (ref. 46) and 4.16,⁴⁷ respectively, showing similar total electron efficiency for acetate and lactate to the extra carbon source from (C₆H₁₂O₆)_n.⁴⁸ CCE of *n*-caproate from lactate also lost one-third of electrons, because lactate was firstly converted to acetate, as illustrated in Table S1.†¹⁷ Therefore, a green strategy of food waste management is first extraction into biochemicals and then application of residual broth in WWTP as an alternative carbon source.

Environmental and engineering implications

Even though the global market of *n*-caproate cannot completely absorb its generation from food waste, this industrial-scale biorefinery plant offers a strategy for the sustainable resource reuse of food waste which is shown to be technically and economically feasible on an industrial scale. Additionally, *n*-caproate can also be a platform compound in fatty acid production through carbon chain elongation as well. For example, the longer acids of caprylate and branched fatty acid of 2-ethylhexanoate can be produced through the CCE process,^{13,25} which would be worthy of further investigation in the future, as higher-valued product and wider outlet of *n*-caproate.

Materials and methods

Detailed workflow of the industrial-scale biorefinery plant

The food waste was daily collected from the living area in a mega-city in the South of China, the physical composition of which is listed in Fig. S1 of the ESI.† The biochemical composition of the feedstock is listed in Table S3.† The biorefinery plant includes a conversion capacity of 150 t d⁻¹ in the pre-treatment and CCE sections. The pre-treatment section crushed the raw food waste into a size less than 10 mm and separated impurities subsequently by the depackage, crush, gravity separation, pulping, hydrocyclone and decanter units shown in Fig. 1. The impurity produced in the pre-treatment



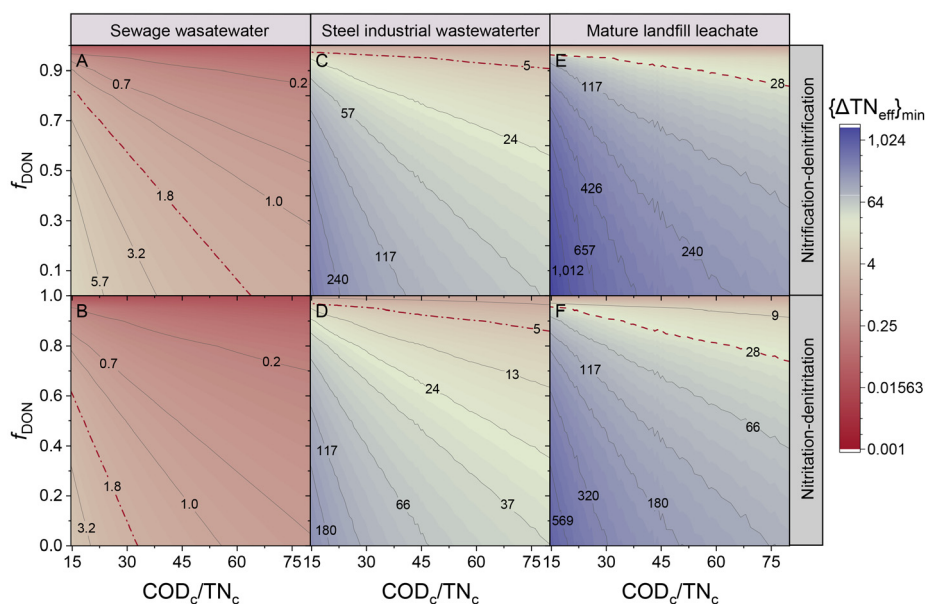


Fig. 4 Effect of properties of mixed MCCA as the carbon source on TN concentration in the effluent WWTP for various wastewater with low COD/TN, such as, sewage wastewater (A and B, 70 mg COD_{WW} per L, 35 mg TN_{WW} per L), steel industrial wastewater (C and D, 30 mg COD_{WW} per L, 800 mg TN_{WW} per L), and mature landfill leachate (E and F, 2800 mg COD_{WW} per L, 3000 mg TN_{WW} per L).

unit was dewatered by a screw press, and the rejected water was recirculated to the depackage unit. The impurity shown in Fig. S1† from the feed stock was incinerated after dewatering. Generally, the CCE section is a bio-membrane reactor coupled with micro-aeration. Pre-treated food waste in the form of slurry was bio-converted into MCCAs in the fed-batch operation mode in the tandem CCE reactors I, II, and III with a hydraulic retention time of 6 days in total. The slurry goes in the three up-flow CCE reactors by gravity with internal recirculation for mixing. The three consecutive chain elongation stages can avoid channeling in a single reactor. The fermented residual was centrifuged to remove the impurities again, and then transported to an ultrafiltration unit by using 1920 m² ceramic membrane with an average pore size of 100 nm. The mixed MCCAs were filtered by gravity in this ultrafiltration unit with continuous crossflow by air to remove the suspended solid. The fermented residual food waste and CCE functional microbes were externally recirculated to the CCE reactors I. Therefore, the solid retention time could be isolated from the hydraulic retention time in the micro-aerobic bio-membrane reactor, and micro-aerobic conditions in CCE reactor I were maintained by the remnant dissolved oxygen in the external recirculation from the ultrafiltration unit.

Performance analysis of the *n*-caproate biorefinery plant

The start-up of the CCE system is not the main focus of this study. For short, the biorefinery plant has been stably operated for one year since the CCE system was commissioned without the inoculum. The sampling sites are remarked in Fig. 1 to show the typical performance. The physical and biochemical composition of food waste was identified. The determined physicochemical properties of the CCE sections include C₂–C₇

organic acids, ethanol, TS, volatile solid, COD, DOC, dissolved Kjeldahl nitrogen, DN, NH₄⁺-N, PO₄³⁻, and microbial diversity based on the CCE processes from food waste. The detailed analysis methods are recorded in the Experimental section of the ESI.†

Solving contradictory equations with Gibbs free energy analysis

Table S1† lists the probable feedstocks, intermediates and products that were related with probable CCE and competitive reactions mediated by lactate and ethanol from food waste.^{25,49} Reaction standard Gibbs free energy $\Delta_r G_m^\ominus$ was calculated for the potential reactions that would occur in CCE reactors I, II and III.⁴³ pH in the CCE reactors was approximately 5.6 in Fig. S5,† so the methanogenesis process was assumed to be inhibited. According to the minimisation of Gibbs free energy, the method of solving contradictory equations was proposed to fit the probable CCE pathways in Fig. 2, because many biochemical fermentation²⁴ and nitrogen metabolism reactions⁵⁰ may simultaneously occur in this complicated CCE system. The input data were the average values of influent concentrations of lactate and ethanol as reactants, and effluent concentrations of mixed MCCAs from CCE reactors as products. The off-gas from CCE reactors cannot be measured on site, so the released CO₂ in Fig. 2 was estimated according to the results of liquid samples.

Estimating the application of mixed MCCAs as a carbon source in wastewater treatment

Besides refinement and purification as chemicals, the mixed MCCAs are the easily biodegradable substrates for the extra carbon source of denitrification and shortcut denitrification in the activated sludge system as an alternative to the chemical



carbon source,³⁷ such as, glucose, sodium acetate, and methanol. Whereas, the protein fraction in food waste would be converted to TN in mixed MCCAs, potentially increasing TN concentration in the final effluent of WWTP.^{44,51} In particular, most of DON in MCCAs typically cannot be converted to N₂ in the activated sludge system during nitrogen removal. Therefore, the ammonification rate of DON is the key to determining the availability of MCCAs as the carbon source. A theoretical eqn (1) was proposed to estimate the relationship between ammonification rate f_{DON} of DON in mixed MCCAs and the probably increased value of TN in the effluent of WWTP $\{\Delta\text{TN}_{\text{eff}}\}_{\text{min}}$ for various kinds of wastewater, such as, sewage wastewater, steel industrial wastewater, and mature leachate. The detailed derivation process is shown by eqn (S1)–(S8) in the ESI.†

$$\{\Delta\text{TN}_{\text{eff}}\}_{\text{min}} = \frac{f_{\text{DON}}(f_{\text{dn}} \cdot \text{TN}_{\text{ww}} - \text{COD}_{\text{ww}})(\text{TN}_{\text{c}} - \text{TN}_{\text{ww}})}{\text{COD}_{\text{c}} - \text{COD}_{\text{ww}} - f_{\text{dn}}(\text{TN}_{\text{c}} - \text{TN}_{\text{ww}})} \quad (1)$$

TN_{ww} and COD_{ww} are the concentrations of TN and easily biodegradable COD in wastewater with low COD/TN. TN_c and COD_c are the concentrations of TN and COD in the mixed MCCAs. f_{dn} represents the coefficient of TN and COD for nitrogen removal. For example, f_{dn} is 5 for nitrification–denitrification, and 3–3.5 for the nitritation and denitritation processes.

Techno-economic evaluation

Based on the performance of this biorefinery plant, techno-economic analysis was conducted to show the operational cost to produce MCCA broth and *n*-caproate from raw food waste. Reduced cost for the production of MCCAs broth was identified, involving reduced energy for heating and free addition of hydroxide ions. Furthermore, *n*-caproate in the broth has not been refined and purified for now, and the mixed MCCAs was applied as an alternative to the chemical carbon source in a sewage wastewater treatment plant. From the broth as the stock, refinement and purification of *n*-caproate can be conducted by the LL-D^{12,35} and ED-PS processes,⁵² facilitating the sustainability of bio-conversion of *n*-caproate from food waste, determined by eqn (2)–(13). The parameters of techno-economic evaluation were recorded in Table S2† according to the realistic consumption of the plant.

1. Costs of consumed tap water P_1

$$P_1 = \frac{Q_{\text{tap water}} \cdot \theta_{\text{tap water}}}{C_{n\text{-caproate}} \cdot Q_{\text{FW}}} \quad (2)$$

$Q_{\text{tap water}}$ is the consumed tap water during the pre-treatment process, which was only used as flushing water for cleaning. $\theta_{\text{tap water}}$ represents the unit price of tap water. $C_{n\text{-caproate}}$ is the concentration of caproate in the broth after the CCE reactor. Q_{FW} is the treatment capacity of this biorefinery plant.

2. Costs of consumed electric power in the pre-treatment and CCE reactor P_2

$$P_2 = \frac{Q_{\text{electric-CCE}} \cdot \theta_{\text{electric}}}{C_{n\text{-caproate}} \cdot Q_{\text{FW}}} \quad (3)$$

$Q_{\text{electric-CCE}}$ is the consumed electric power during the pre-treatment and CCE processes. θ_{electric} represents the unit price of electric power.

3. Saving costs of steam and chemicals

$$P_3 = -\frac{C_{\text{p,water}} \cdot \rho_{\text{FW}} \cdot (1 + \eta) \cdot (t_2 - t_1) \cdot \theta_{\text{steam}}}{C_{n\text{-caproate}} \cdot (C_{\text{v,water}} - t_2 \cdot C_{\text{p,water}})} \quad (4)$$

$$P_4 = -\frac{R_{\text{NaOH}} \cdot \theta_{\text{NaOH}}}{C_{n\text{-caproate}}} \quad (5)$$

$$P_5 = -\frac{R_{\text{ethanol}} \cdot \theta_{\text{ethanol}}}{C_{n\text{-caproate}}} \quad (6)$$

Compared with the previous pilot-scale research studies,^{35,37} P_3 , P_4 , and P_5 are the saving costs of steam, NaOH and ethanol in this biorefinery plant, respectively. ρ_{FW} is the density of the food waste. θ_{steam} , θ_{NaOH} , and θ_{ethanol} are the unit prices of steam, NaOH, and ethanol, respectively. η is the excess ratio of steam, and η is 15% in this plant. t_1 and t_2 are the primitive and heated temperatures of food waste. $C_{\text{p,water}}$ and $C_{\text{v,water}}$ are the constant-pressure specific heat capacity of water and enthalpy of evaporation of water, respectively. R_{NaOH} and R_{ethanol} are the dosage ratios of NaOH under pH conditions and electron donor in per tonne broth, respectively.^{31,35}

4. Estimated costs of refinement and purification of *n*-caproate by the LL-D process

$$P_6 = \frac{R_{\text{HCl}} \cdot \theta_{\text{HCl}}}{C_{n\text{-caproate}}} \quad (7)$$

$$P_7 = \frac{R_{\text{sol}} \cdot Q_{\text{sol}} \cdot \theta_{\text{sol}}}{C_{n\text{-caproate}} \cdot Q_{\text{MCCAs}}} \quad (8)$$

$$P_8 = \frac{Q_{\text{sol}} \cdot C_{\text{v,sol}} \cdot \theta_{\text{sol}}}{C_{n\text{-caproate}} \cdot C_{\text{v,water}} \cdot Q_{\text{MCCAs}}} \quad (9)$$

P_6 , P_7 , and P_8 are the estimated costs of HCl, wasted solvent of LL and energy of distillation in refinement and purification processes, respectively. R_{sol} is the loss ratio of the solvent in the LL process. R_{HCl} is the dosage ratio of HCl. θ_{HCl} and θ_{sol} are the unit price of HCl and wasted solvent of LL. $C_{\text{v,sol}}$ is the enthalpy of evaporation of the solvent of LL. Q_{sol} and Q_{MCCAs} is the amount of solvent of LL and produced mixed MCCAs after CCE.²⁷

5. Estimated costs of refinement and purification of *n*-caproate by the ED-PS process P_9

$$P_9 = \frac{Q_{\text{electric-ED-PS}} \cdot \theta_{\text{electric}}}{C_{n\text{-caproate}} \cdot Q_{\text{MCCAs}}} \quad (10)$$

$Q_{\text{electric-ED-PS}}$ is the consumed electric power during the ED-PS process.⁵²

6. Sensitivity analysis

S is the result of sensitivity analysis in the neighbourhood of x .

$$S = \frac{\partial y}{\partial x} \cdot \frac{x}{y} \quad (11)$$



The sensitivity of P_1 – P_9 is a constant value except for P_3 .

$$\frac{\partial P_3}{\partial t_1} \cdot \frac{t_1}{P_3} = \frac{-t_1}{t_2 - t_1} \quad (12)$$

$$\frac{\partial P_3}{\partial t_2} \cdot \frac{t_2}{P_3} = \frac{t_2(C_{v,water} - t_2 \cdot C_{p,water})}{(t_2 - t_1)(C_{v,water} - t_1 \cdot C_{p,water})} \quad (13)$$

Conclusions

An industrial-scale biorefinery plant was reported for the production of *n*-caproate in broth from food waste. The conclusions are as follows:

(1) Food waste was successfully converted to *n*-caproate with the volumetric production rate of 3.8 kg *n*-caproate per (m³ d), comparable with previous bench-scale results.

(2) This integrated system to gear the anaerobic bio-membrane reactor and micro-aeration technology could simultaneously suppress the propionic acid fermentation as a competitive reaction, and ammonify the proteins to avoid the addition of NaOH.

(3) The avoidable input of NaOH, ethanol and heat energy significantly enhanced the technical and economic feasibility to produce *n*-caproate from food waste on the industrial scale, and can offset the high cost of purification of *n*-caproate.

(4) A theoretical model was developed to estimate the performance for application of mixed MCCAs as a carbon source in wastewater treatment as a cascade management strategy, and further stress the significance of ammonifying the proteins during the CCE process.

Author contributions

F.L., H.Z., P.H., Y.W., and J.Q. designed research; Y.W., X.H., J.L., and J.Q. performed research; J.Q. analysed data; B.X. and P.H. supervised research; and J.Q., F.L. and N.L. wrote the paper.

Data availability

The data supporting this article have been included within this article and the ESI.†

Conflicts of interest

There are no conflicts to declare.

Acknowledgements

This article is in memory of Dr Wenhao Han for his early idea in production of MCCAs from food waste mediated by lactate, and the idea was realised in this industrial-scale plant. The authors appreciate the financial support from the National

Natural Science Foundation of China (51622809 and 51878471), and the Postdoctoral Fellowship Program of CPSF under Grant Number GZB20240537.

References

- 1 United Nations Environment Programme, *Food Waste Index Report 2024. Think Eat Save: Tracking Progress to Halve Global Food Waste*, 2024.
- 2 J. Zhu, Z. Luo, T. Sun, W. Li, W. Zhou, X. Wang, X. Fei, H. Tong and K. Yin, *Nat. Food*, 2023, **4**, 247–256.
- 3 M. F. Bellemare, *Nat. Food*, 2023, **4**, 547–547.
- 4 L. Xue, X. Liu, S. Lu, G. Cheng, Y. Hu, J. Liu, Z. Dou, S. Cheng and G. Liu, *Nat. Food*, 2021, **2**, 519–528.
- 5 Y. Guo, H. Tan, L. Zhang, G. Liu, M. Zhou, J. Vira, P. G. Hess, X. Liu, F. Paulot and X. Liu, *Nat. Food*, 2023, **4**, 686–698.
- 6 L. T. Angenent, I. Casini, U. Schröder, F. Harnisch and B. Molitor, *Energy Environ. Sci.*, 2024, **17**, 3682–3699.
- 7 C. L. Mao, J. Byun, H. W. MacLeod, C. T. Maravelias and G. A. Ozin, *Joule*, 2024, **8**, 1224–1238.
- 8 Y. Wang, R. Wang, K. Tanaka, P. Ciais, J. Penuelas, Y. Balkanski, J. Sardans, D. Hauglustaine, W. Liu, X. Xing, J. Li, S. Xu, Y. Xiong, R. Yang, J. Cao, J. Chen, L. Wang, X. Tang and R. Zhang, *Nature*, 2023, **619**, 761–767.
- 9 E. S. Pattison, *Fatty acids and their industrial applications*, Marcel Dekker, 1968.
- 10 R. Höfer, *Renewable Resources for Surface Coatings, Inks and Adhesives*, Royal Society of Chemistry, 2022.
- 11 E. d. Boer and J. d. Boer, *Production of volatile fatty acids in biorefineries. Chpt. 6 in: Waste Biorefinery: Value Addition through Resource Utilization*, Elsevier, 2021.
- 12 K. J. J. Steinbusch, H. V. M. Hamelers, C. M. Plugge and C. J. N. Buisman, *Energy Environ. Sci.*, 2011, **4**, 216–224.
- 13 M. T. Agler, C. M. Spirito, J. G. Usack, J. J. Werner and L. T. Angenent, *Energy Environ. Sci.*, 2012, **5**, 8189.
- 14 Y. Pu, Y. Wang, G. Wu, X. Wu, Y. Lu, Y. Yu, N. Chu, X. He, D. Li, R. J. Zeng and Y. Jiang, *Environ. Sci. Technol.*, 2024, **58**, 7445–7456.
- 15 L. T. Angenent, H. Richter, W. Buckel, C. M. Spirito, K. J. J. Steinbusch, C. M. Plugge, D. P. B. T. B. Strik, T. I. M. Grootsholten, C. J. N. Buisman and H. V. M. Hamelers, *Environ. Sci. Technol.*, 2016, **50**, 2796–2810.
- 16 A. Duber, L. Jaroszynski, R. Zagrodnik, J. Chwialkowska, W. Juzwa, S. Ciesielski and P. Oleskiewicz-Popiel, *Green Chem.*, 2018, **20**, 3790–3803.
- 17 C. M. Spirito, H. Richter, K. Rabaey, A. J. M. Stams and L. T. Angenent, *Curr. Opin. Biotechnol.*, 2014, **27**, 115–122.
- 18 S. Shrestha, S. Xue and L. Raskin, *Environ. Sci. Technol.*, 2023, **57**, 3369–3379.
- 19 H. W. Duan, P. J. He, L. M. Shao and F. Lü, *ISME J.*, 2021, **15**, 2906–2919.
- 20 L. A. Kucek, M. Nguyen and L. T. Angenent, *Water Res.*, 2016, **93**, 163–171.



- 21 E. R. Nie, P. J. He, J. L. Zou, H. Zhang and F. Lu, *J. Cleaner Prod.*, 2022, **352**, 131603.
- 22 L. Day, J. A. Cakebread and S. M. Loveday, *Trends Food Sci. Technol.*, 2022, **119**, 428–442.
- 23 W. H. Han, P. J. He, L. M. Shao and F. Lu, *Appl. Environ. Microbiol.*, 2018, **84**, e01614–e01618.
- 24 M. Coma, R. Vilchez-Vargas, H. Roume, R. Jauregui, D. H. Pieper and K. Rabaey, *Environ. Sci. Technol.*, 2016, **50**, 6467–6476.
- 25 K. D. de Leeuw, C. J. N. Buisman and D. P. B. T. B. Strik, *Environ. Sci. Technol.*, 2019, **53**, 7704–7713.
- 26 M. Roghair, T. Hoogstad, D. P. B. T. B. Strik, C. M. Plugge, P. H. A. Timmers, R. A. Weusthuis, M. E. Bruins and C. J. N. Buisman, *Environ. Sci. Technol.*, 2018, **52**, 1496–1505.
- 27 W.-S. Chen, D. P. B. T. B. Strik, C. J. N. Buisman and C. Kroeze, *Environ. Sci. Technol.*, 2017, **51**, 7159–7168.
- 28 L. Wu, W. Wei, Z. Chen, X. Shi, J. Qian and B.-J. Ni, *Chem. Eng. J.*, 2024, **483**, 149236.
- 29 A. Menon and J. G. Lyng, *Rev. Environ. Sci. Biotechnol.*, 2020, **20**, 189–208.
- 30 J. M. Carvajal-Arroyo, S. J. Andersen, R. Ganigué, R. A. Rozendal, L. T. Angenent and K. Rabaey, *Chem. Eng. J.*, 2021, **416**, 127886.
- 31 C. A. Contreras-Dávila, V. J. Carrión, V. R. Vonk, C. N. J. Buisman and D. P. B. T. B. Strik, *Water Res.*, 2020, **169**, 115215.
- 32 R. Zagrodnik, A. Duber, M. Łężyk and P. Oleskowicz-Popiel, *Environ. Sci. Technol.*, 2020, **54**, 5864–5873.
- 33 E. Noor, E. Eden, R. Milo and U. Alon, *Mol. Cell*, 2010, **39**, 809–820.
- 34 T. Hino and S. Kuroda, *Appl. Environ. Microbiol.*, 1993, **59**, 255–259.
- 35 X. Zhu, H. Huang, Y. He, X. Wang, J. Jia, X. Feng, D. Li and H. Li, *Bioresour. Technol.*, 2022, **366**, 128154.
- 36 E. R. B. Moore, F. Salvà-Serra, D. Jaén-Luchoro, M. L. Hammarström, S. Hammarström, M. Hedberg and A. Oren, in *ergey's Manual of Systematics of Archaea and Bacteria*, 2021, pp. 1–15, DOI: [10.1002/9781118960608.gbm02007](https://doi.org/10.1002/9781118960608.gbm02007).
- 37 I. Owusu-Agyeman, B. Bedaso, C. Laumeier, C. Pan, A. Malovanyy, C. Baresel, E. Plaza and Z. Cetecioglu, *Renewable Sustainable Energy Rev.*, 2023, **175**, 113163.
- 38 H. Wang, Y. Gu, W. Zhou, D. Zhao, Z. Qiao, J. Zheng, J. Gao, X. Chen, C. Ren and Y. Xu, *Appl. Environ. Microbiol.*, 2021, **87**, e01203–e01221.
- 39 S. Fu, S. Lian, I. Angelidaki and R. Guo, *Trends Biotechnol.*, 2023, **41**, 714–726.
- 40 M. Zhu, F. Lü, L.-P. Hao, P.-J. He and L.-M. Shao, *Waste Manage.*, 2009, **29**, 2042–2050.
- 41 Q.-L. Wu, K.-X. Yuan, W.-T. Ren, L. Deng, H.-Z. Wang, X.-C. Feng, H.-S. Zheng, N.-Q. Ren and W.-Q. Guo, *Engineering*, 2024, **35**, 180–190.
- 42 X. Gu, J. Sun, T. Wang, J. Li, H. Wang, J. Wang and Y. Wang, *Bioresour. Technol.*, 2024, **402**, 130782.
- 43 R. Kleerebezem and M. C. M. Van Loosdrecht, *Crit. Rev. Environ. Sci. Technol.*, 2010, **40**, 1–54.
- 44 H. D. Hu, Y. J. Shi, K. W. Liao, H. J. Ma, K. Xu and H. Q. Ren, *Water Res.*, 2019, **162**, 87–94.
- 45 H. Z. Cheng, J. Q. You, S. J. Ma, K. W. Liao, H. D. Hu and H. Q. Ren, *Environ. Sci. Technol.*, 2024, **58**, 2870–2880.
- 46 Y. Mokhayeri, A. Nichols, S. Murthy, R. Riffat, P. Dold and I. Takacs, *Water Sci. Technol.*, 2006, **54**, 155–162.
- 47 M. Sage, G. Daufin and G. Gésan-Guiziou, *Water Res.*, 2006, **40**, 2747–2755.
- 48 D. M. Schütterle, R. Hegner, M. Temovska, A. E. Ortiz-Ardila and L. T. Angenent, *Water Res.*, 2024, **250**, 121045.
- 49 S. J. Ge, J. G. Usack, C. M. Spirito and L. T. Angenent, *Environ. Sci. Technol.*, 2015, **49**, 8012–8021.
- 50 M. M. M. Kuypers, H. K. Marchant and B. Kartal, *Nat. Rev. Microbiol.*, 2018, **16**, 263–276.
- 51 X. Cui, J. Q. You, K. W. Liao, L. L. Ding, H. D. Hu and H. Q. Ren, *Environ. Sci. Technol.*, 2024, **58**, 4648–4661.
- 52 J. Xu, J. J. L. Guzman and L. T. Angenent, *Environ. Sci. Technol.*, 2020, **55**, 634–644.

